European Conference on Optical Communication (ECOC) 2022 © Optica Publishing Group 2022

Distributed Polarization Dependent Loss Monitoring using Polarization Resolved Pilot Tone

Zhiping Jiang(1), Xiang Lin(1)

(1) Huawei Technologies Canada, 303 Terry Fox Drive, Ottawa, Canada, zhiping.jiang@huawei.com

Abstract *We propose and experimentally demonstrate a novel scheme to monitor polarization dependent loss of lightpath segments distributedly using polarization resolved pilot tone technology. Better than 0.1 dB accuracy is achieved.*

Introduction

Accurate characterization of lightpath (LP) components and parameters uncertainties is desired to more accurately allocate system operating margins [1-7]. Among various link parameters, polarization dependent loss (PDL) caused by the devices along the link is a major impairment in polarization multiplexed (PM) systems. Different methods have been proposed to monitor PDL of link segment [8, 9]. In [8], the signal-to-noise ratio (SNR) distribution induced by PDL is proposed to estimate the ROADM (reconfigurable optical add-drop multiplexer) PDL. The approach was verified in simulation, but its validality in real link has yet to be confirmed as there are other factors affecting SNR in addition to PDL. In [9], amplitude modulation pilot tone (PT) was proposed to monitor the accumulated PDL from transmitter to PT detector. However, the acutally monitored is the PDL-induced orthogonal polarization power ratio (OPPR) rather than PDL itself. OPPR is equal to PDL only if the signal's polarization is aligned with PDL's principal axis. There still lacks effective distributed PDL monitoring capability in real fiber optical links.

In this paper, we propose to use polarization resolved PT technology to monitor the PDL value of link segment distributedly. The proposed scheme is first shown mathmatically, and is then verified by simulations and experiments.

Monitoring Principle

The basic principle is illustrated in Fig. 1. In the PM transmitter (Tx), PTs with different frequencies are applied to each polarization. Without lossing generality for the purpose of PDL monitoring, the link is simplified to SOP rotations R_1 and R_2, as well as PDL elements PDL_1 and PDL_2. PT detectors PTD₁ and PTD₂ are placed along the link to monitor the OPPR ΔP_1 and ΔP_2, respectively. For PT detection, a small portion of signal power is tapped. In deployed optical fiber communication systems, random SOP rotation occurs due to environment change, resulting in the OPPR change [10]. PDL can then be obtained by using the extreme values in OPPR measurements, just as in the typical PDL measurement [11].

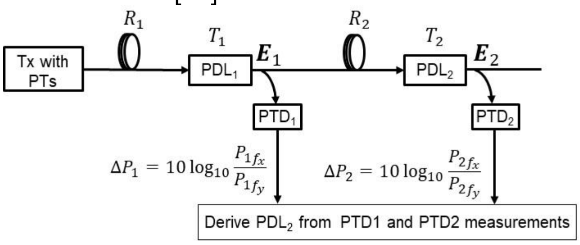

Fig. 1: Schematic of distributed PDL monitoring using polarization resolved pilot tone.

For simplicity, only two lightpath segments (delineated by adjacent PTDs) are shown in Fig. 1. The PDL of the lightpath segment between PTD_1 and PTD_2 is obtained by the extreme values in the difference waweform $\Delta P_{21}(t) = \Delta P_2(t) - \Delta P_1(t)$. Both $\Delta P_1(t)$ and $\Delta P_2(t)$ are in dB unit. Note that in a lightpath with multiple PTDs, the PDL value of all segments can be obtained, providing distributed monitoring capability.

Polarization resolved pilot tone: As explained in [5], amplitude modulation PT can be easily applied in the Tx DSP with no additional cost. To differentiate each polarization stream, different PT frequencies are used for orthogonal polarizations. Let $E_{0x}(t)$ and $E_{0y}(t)$ be the complex electrical field for X/Y polarizations without PT. With PT modulation, they become

$$E_{0x}(t)(1 + m_x\cos(2\pi f_x t)) \,, \tag{1a}$$
$$E_{0y}(t)(1 + m_y\cos(2\pi f_y t)) \,, \tag{1b}$$

where f_x and f_y are the PT frequencies for X and Y polarizations, respectively; m_x and m_y the corresponging modulation index. This polarization resolved PT enables separate monitoring of the signal power in each Tx polarization without using complex polarization diversity detection.

OPPR detection: After passing SOP rotations and PDL elements between the the Tx and monitoring point, the signal that arrives at the

978-1-6654-3868-1/21/$31.00 ©2022 IEEE

monitoring point is expressed as

$$\begin{pmatrix} E_x(t) \\ E_y(t) \end{pmatrix} = \mathbf{H} \begin{pmatrix} E_{0x}(t)(1+m_x\cos(2\pi f_x t)) \\ E_{0y}(t)(1+m_y\cos(2\pi f_y t)) \end{pmatrix}, \quad (2)$$

where $\mathbf{H}$ represents the channel response of *N* cascaded SOP rotations and PDLs, and is given by

$$\mathbf{H} = \prod_{i=1}^{N} \begin{pmatrix} (1+\gamma_i)^{1/2} & 0 \\ 0 & (1-\gamma_i)^{1/2} \end{pmatrix} \begin{pmatrix} e^{j\phi_i}\cos\theta_i & -e^{-j\phi_i}\sin\theta_i \\ e^{j\phi_i}\sin\theta_i & e^{-j\phi_i}\cos\theta_i \end{pmatrix}. \quad (3)$$

In (3), γ_i is PDL parameter for the *i*th PDL element (its PDL value in dB is defined as $10\log_{10}(\frac{1+\gamma_i}{1-\gamma_i})$), ϕ_i and θ_i are angles descrbing the *i*th SOP rotation.

In PT detection, the optical power waveform

$$I(t) = |E_x(t) + E_y(t)|^2 \quad (4)$$

is converted into electrical domain by a photodetector and then digitized by an ADC. Inserting (2) to (4), one can find that the magnitudes of the pilot tones with frequencies f_x and f_y are

$$P_{f_x} = (|H_{11}|^2 + |H_{21}|^2)\, m_x \overline{|E_{0x}(t)|^2} \quad , \quad (5a)$$

$$P_{f_y} = (|H_{12}|^2 + |H_{22}|^2)\, m_y \overline{|E_{0y}(t)|^2} \quad , \quad (5b)$$

where $H_{u,v}$ represents the element in the *u*th row and *v*th column of **H** ($u, v \in \{1,2\}$), and the average time window is the integration time for one PT detection period, which is in the order of milliseconds. **H** is assumed invariant during one PT measurement. In deriving (5), the high order terms containing m_x^2, m_y^2 are neglected, and the cross terms containing $E_{0x}(t)E_{0y}^*(t)$, $E_{0x}^*(t)E_{0y}(t)$ are averaged out to zero. The OPPR in dB unit is given by

$$\Delta P = 10\log_{10}\left(\frac{(|H_{11}|^2+|H_{21}|^2)\, m_x\overline{|E_{0x}(t)|^2}}{(|H_{12}|^2+|H_{22}|^2)\, m_y\overline{|E_{0y}(t)|^2}}\right). \quad (6)$$

$\frac{m_x\overline{|E_{0x}(t)|^2}}{m_y\overline{|E_{0y}(t)|^2}}$ is pilot tone ratio at the Tx output and is known. It is set to 1 for simplicity. When $N = 1$, one can derive the OPPR in dB by using (2), (3), and (6), and the derived result is

$$\Delta P_1 = 10\log_{10}\frac{1+\gamma_1\cos2\theta_1}{1-\gamma_1\cos2\theta_1} \quad . \quad (7)$$

As is seen the PDL paramter γ_1 can be obtained when the OPPR achieves its maximum ($\theta_1 = 0$) or minimum ($\theta_1 = \pi/2$).

PDL monitoring of lighpath segment: The PDL of any lightpath segment between two PTDs can be obtained by monitoring their OPPRs, as the extremes in the OPPR *difference* is linked to the segment PDL only. We consider the case of *N*=2 without loss of generality. It can be shown that the OPPR after the second PDL element is expressed as

$$\Delta P_2 = 10\log_{10}\frac{1+\gamma_2\cos2\theta_2}{1-\gamma_2\cos2\theta_2} + \Delta P_1. \quad (8)$$

The OPPR difference ($\Delta P_2 - \Delta P_1$) is only determined by θ_2 and γ_2. This is because by subtracting the OPPR at the PDL_1 output, any power imbalance in two polarizations up to that point is normalized out, the OPPR difference depends only on the PDL and SOP between those two locations.

We simulated the configuration in Fig. 1 with 0.3 dB for PDL_1, 0.5 dB for PDL_2, and random SOP rotations R_1, R_2. Two OPPR waveforms at PTD_1 and PTD_2 are shown in the upper subfigure of Fig. 2. ΔP_1 is between -0.3 and +0.3 dB, because only PDL1 is involved. For PTD_2, ΔP_2 is between -0.8 and +0.8 dB, because both PDL_1 and PDL_2 contribute to its OPPR. The difference OPPR is shown in the lower subfigure of Fig. 2, where the extreme values (-0.5dB, +0.5 dB) depend on PDL_2 only. Note that it is less likely for ΔP_2 to reach extremes as it depends on both SOP rotation R_1 and R_2. In addition, the randomness of the OPPR difference depends on R_2 only, not on R_1.

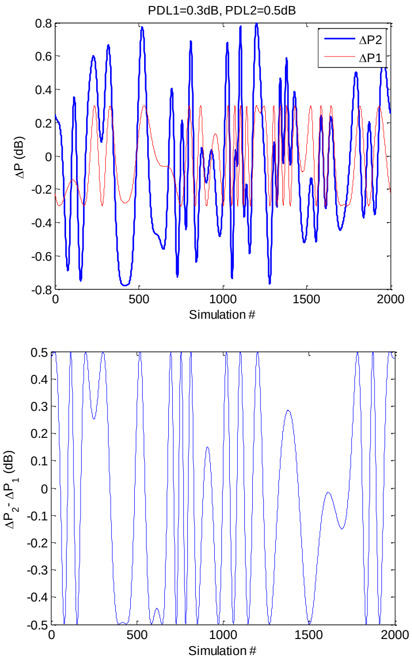

Fig. 2: Simulation results.

SOP speed discussion: The proposed method relies on the assumption that the SOP does not change in one PT measurement, but covers all possible states after sufficiently large number of measurements. As shown in [10], the monitored end-to-end PDL of link exhibits small change within a relatively short period (in the order of hours), but it changes substantially when the monitoring period is longer (days or weeks). Therefore, the above assumption could be satisfied. In the case when SOP does change significantly within one PT measurement, the measurement will not affect the PDL monitoring result, as only the extreme values in OPPR is used to obtain the PDL value.

Experimental Demonstration

To further verify the concept, an experimental setup shown in Fig. 3 is used. A commercialized Tx generates PM-QAM signal with PT of frequencies of 43.36 and 44 MHz on orthogonal polarizations. A variable optical attenuator (VOA) is introduced to provide power variation to mimic real link condition. Two SOP scramblers are used to introduce random SOP rotation. Note that this is only for lab confirmation, in the deployed optical networks, natural SOP rotations due to environment change is used. The values of the PDL emulators are also measured using typical method, and treated as the true PDL. The PT detection is done by the PTD embedded in EDFA cards.

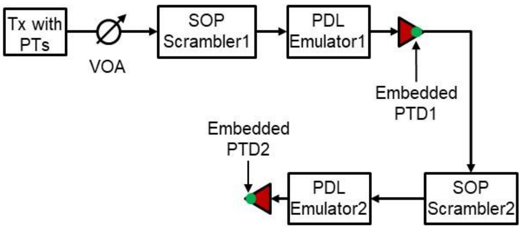

Fig. 3: Experimental setup.

PTD performance analysis: In optical networks, although channel power fluctuation happens due to many factors, such as the fiber loss evolution and EDFA gain change, the proposed PDL monitoring is not affected by such power fluctuation. This benefit comes from the fact that OPPR is a relative power measurement of the orthogonal polarizations. To verify this, the OPPR is measured without SOP rotation while more than 2 dB power fluctuation is introduced. As shown in Fig. 4, while the tone powers vary by more than 2 dB, the power difference between them is very stable, with less than 0.1 dB peak to peak variation. This indicates that better than 0.05 dB PDL estimation accuracy can be achieved.

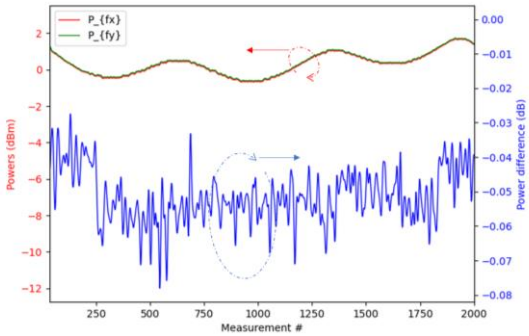

Fig. 4: Optical power of individual tones and their difference.

PDL monitoring performance: Since the PDL monitoring of the first PDL element is straightforward and relatively trivial, we demonstrate the monitoring of the second PDL element. 5 different PDL values are measured. The results are shown in Fig. 5, where the straight dash line indicates the set PDL values. The error is less than 0.05 dB, consistent with the OPPR measurement uncertainty.

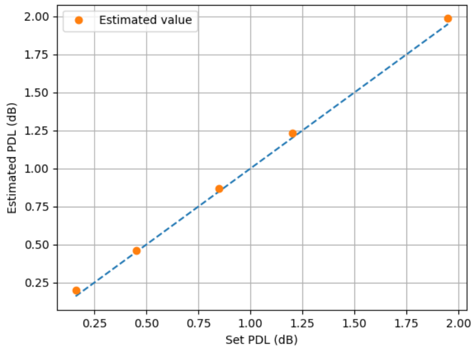

Fig. 5: Monitored PDL value vs. set PDL.

In another demonstration, the PDL of a 1x20 wavelength selective switch (WSS) is monitored, as WSS is the major PDL contributor in the link. The second PDL emulator in Fig. 3 is replaced by the WSS under test. Figure 6 shows the monitored PDL as a function of wavelength for 3 ports, port 1, 12, and 20 (black solid curves). As comparison, the PDL values obtained with typical measurement method are also shown (red dash-dotted curves). The mean values of the monitoring errors are 0.036 dB, 0.052 dB, and 0.063 dB for Port 1, 12, and 20, respectively. This demonstration shows the capability of monitoring the PDL of link components for each signal at its wavelength.

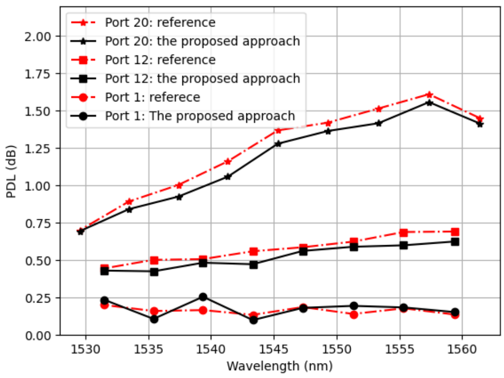

Fig. 6: Monitored WSS PDL vs. wavelength.

Conclusion

Polarization resolved PT is proposed to monitor PDL of link segments. The proposed scheme provides accurate, distributed, and wavelength-dependent PDL monitoring capability, leading to more accurate margin allocation. With the low cost PT technology already widely-deployed in the optical networks, it is essentially free. This monitoring capability opens up opportunities for PDL mitigation in the photonic layer.

References

[1] L. Velasco, *et al.*, “Designing, operating, and reoptimizing elastic optical networks,” *J. Light. Technol.*, vol. 35, no. 3, pp. 513–526, Feb. 2017.

[2] Y. Pointurier, “Design of low-margin optical networks,” *J. Opt. Commun. Netw.*, vol. 9, pp. A9–A17, 2017.

[3] Z. Dong, “Optical performance monitoring: A review of current and future technologies,” *J. Lightw. Technol.*, vol. 34, no. 2, pp. 525–543, Jan. 2016.

[4] Z. Jiang, *et al.*, “DSP enabled, amplitude modulation pilot tone based optical performance monitoring in coherent systems,” *in Proc. Eur. Conf. Opt. Commun.*, Bordeaux, France, Sept. 2021, pp. 1-3.

[5] Z. Jiang, *et al.*, “Direct nonlinear noise monitoring for in-service signals in coherent systems,” *in Proc. Eur. Conf. Opt. Commun.*, Brussels, Belgium, Sept. 2020, pp. 1-3.

[6] Z. Jiang, *et al.*, “Progresses of pilot tone based optical performance monitoring in coherent systems,” *J. Lightw. Technol.*, 2022, early access, DOI: 10.1109/JLT.2022.3146232.

[7] X. Lin, *et al.*, “A non-data-aided OSNR estimation algorithm for coherent optical fiber communication systems employing multilevel constellations,” *J. Lightw. Technol.*, vol. 37, no. 15, pp. 3815–3825, Jun. 2019.

[8] J. Girard-Jollet, *et al.*, “Estimating network components polarization-dependent loss using performance statistical measurements,” *in Proc. Eur. Conf. Opt. Commun.*, Bordeaux, France, Sept. 2021, pp. 1-3.

[9] B. Kozichi, “Monitoring of orthogonal polarization power ratio due to PDL using intensity tones in polarization multiplexed signals,” *in Proc. Opt. Fiber Commun. Conf.*, San Diego, CA, Mar. 2011, pp. 1-3

[10] L. E. Nelson *et al.*, “Statistics of polarization dependent loss in an installed long-haul WDM system,” *Opt. Express*, vol. 19, no. 7, pp. 6790–6796, Mar. 2011.

[11] “Application Note for PDL Measurement,” https://lunainc.com/sites/default/files/assets/files/resource-library/Application-Note-for-PDL-Measurement.pdf.